Nanofiller Fibre-Reinforced Polymer Nanocomposites

J. Njuguna[1,*], K. Pielichowski[2] and S. Desai[1]

[1]Department of Materials, Cranfield University, Bedfordshire MK43 0AL, UK
[2]Department of Chemistry and Technology of Polymers, Cracow University of Technology, ul. Warszawska 24, 31-155 Kraków, Poland.

Abstract

In this work, the technology of nano and micro-scale particle reinforcement concerning various polymeric fibre-reinforced systems including polyamides (PA), polyesters, polyurethanes, polypropylenes and high performance/temperature engineering polymers such as polyimide (PI), poly(ether ether ketone) (PEEK), polyarylacetylene (PAA) and poly p-phenylene benzobisoxazole (PBO) is reviewed. When the diameters of polymer fibre materials are shrunk from micrometers to submicrons or nanometers, there appear several unique characteristics such as very large surface area to volume ratio (this ratio for a nanofibre can be as large as 10^3 times of that of a microfibre), flexibility in surface functionalities and superior mechanical performance (such as stiffness and tensile strength) compared with any other known form of the material. However, nanoparticle reinforcement of fibre reinforced composites has been shown to be a possibility, but much work remains to be performed in order to understand how nanoreinforcement results in dramatic changes in material properties. The understanding of these phenomena will facilitate their extension to the reinforcement of more complicated anisotropic structures and advanced polymeric composite systems.

Keywords: Fibre-reinforced composites, Nanocomposites, Carbon nanotubes, Nanoclay, Nanofibres

[*] Corresponding author: j.njuguna@cranfield.ac.uk, Tel. +44 1234 754186, Fax: +44 1234 752473 (J. Njuguna).

1. Introduction

Increasing demands for special materials led to the conception of composites, since valuable properties of different types of materials can be combined. Nowadays, engineering materials at the atomic and molecular levels are creating a revolution in the field of materials and processing [1-3]. The discovery of new nanoscaled materials such as nanoclays, carbon nanotubes, and others offer the promise of a variety of new composites, adhesives, coatings and sealant materials with specific properties [4-9]. Nano-particles are presently considered to be high-potential filler materials for the improvement of mechanical and physical polymer properties. The nanometric size, leading to huge specific surface areas of up to more than 1000 m^2/g, and their unique properties (of at least some of these nano-particles) have caused intensive research activities in the fields of natural and engineering sciences.

The concept of combining nanocomposites as matrix material with fibre reinforcement in a new three-phase composite reinforcement has been shown to be very successful. Lighter, thinner, stronger and cheaper structures are the goals of materials science and engineering applications nowadays. In particular, the key goal is to increase the matrix dominated flexural (and compressive) strength by increasing the matrix modulus. As shown in this work, this has been achieved with several types of polymers nanocomposites in combination with fibres such as glass and carbon fibres.

In addition to improving recyclability of the fibre reinforced composites, the improved properties of the nanocomposite matrix material may upgrade the properties of relatively low cost composites up to the level of high performance composites and further increase the temperature resistance of existing high-performance composites. The added cost of the nano-filled matrix can be small due to the low amounts of filler necessary for a significant improvement. Another interesting property is that film extrusion (and probably also film blowing) with low molecular weight (MW) polymers is much easier with nanocomposites due to the altered melt flow behaviour. For instance, a low MW nanocomposite can replace a high MW unfilled polyamide 6 (PA 6). The other advantage of the use of polymer nanocomposites compared to the use of different polymers to improve the high temperature behaviour of fibre composites is that the properties can be improved without any change in the melting temperature and processing conditions [10, 11]. Polymers such as PA 6 can be used as matrix material at temperatures up to 50 °C higher at the same composite strength without changes in the impregnation and forming temperature. However, a common drawback is the fact that the flow properties of the

nanocomposites often lead to difficult fibre bundle impregnation, void formation and reduced adhesion. All these factors often lead to a reduction of the strength instead of the expected increase, and therefore, the nanocomposites used in these fibre composites have to be carefully selected.

In the last two decade, some studies have shown the potential improvement in properties and performances of fibre reinforced polymer matrix materials in which nano and micro-scale particles were incorporated. Nano fibre composites have been processed using a variety of matrices. For general fibre processing technology, reader is referred elsewhere. In the followings is the review of this technology of nano- and micro-scale particle reinforcement concerning various polymeric fibre-reinforced systems including polyamide (PA), polyester, polyurethane, hydroxyapatite (HA) and high performance/temperature engineering polymers such as polyimide (PI), poly(ether ether ketone) (PEEK), polyarylacetylene (PAA) and poly p-phenylene bezobisoxazole (PBO).

2. Fibre reinforced nanocomposites

2.1 Polyamide nanocomposites

In the early 90s, Toyota Research group synthesized Nylon-6-based clay nanocomposites that demonstrated the first use of nanoclays as reinforcement of polymer systems. They concluded that nanoclays not only influenced the crystallization process, but that they were also responsible for morphological changes. Recognizing these benefits, many researchers, using a variety of clays and polymeric matrices, have produced nanocomposites with improved properties. For instance, Liu *et al.* [12] reported that there was an increase in storage elastic modulus of 100% when clay content was up to 8 wt.% in comparison with net PA 11. Usuki *et al.* [13] polymerized ε-caprolactam in the interlayer of an organoclay to form a nanocomposite. This material contained only 4.2 wt.% clay and had a 50% increase in strength, an increase in the heat distortion temperature of 80 °C, a 100% increase in tensile modulus, and a 20% increase in impact resistance.

The electrospun nanocomposite fibres have great potential for the applications where both high surface-to-volume ratio and strong mechanical properties are required such as the high-performance filters and fibre reinforcement materials. Since the mechanical properties of fibres in general improve substantially with decreasing fibre diameter, there is considerable interest in the

development of continuous electrospun polymer nanofibres. In this respect, Lincoln *et al.* [14] reported that the degree of crystallinity of PA-6 annealed at 205 °C increased substantially with the addition of montmorillonite (MMT). This implied that the silicate layers could act as nucleating agents and/or growth accelerators. In contrast, the study of Fong *et al.* [15] showed a very similar overall degree of crystallinity for electrospun PA-6 and PA-6/Cloisite-30B nanocomposite fibres containing 7.5 wt.% of organically-modified MMT (OMMT) layers. Fornes and Paul [16] have found that OMMT layers could serve as nucleating agents at 3% concentration in PA-6/OMMT nanocomposite but retarded the crystallization of PA 6 at a higher concentration of around 7%. In addition, the differences in the molecular weight of PA 6 and the solvent used for electrospinning were also expected to have different impacts on the mobility of PA-6 molecular chains and the interactions between the PA-6 chains and OMMT layers, which may also affect the crystallization behaviour of PA-6 molecules during the electrospinning. Li *et al.* [17] manufactured PA-6 fibres and nanocomposite fibres with average diameters around 100 nm by electrospinning using 88% aqueous formic acid as the solvent. The addition of OMMT layers in the PA-6 solution increased the solution viscosity significantly and changed the resulting fibre morphology and sizes. TEM images of the nanocomposite fibres and ultra-thin fibre sections and the WAXD results showed that OMMT layers were well exfoliated inside the nanocomposite fibres and oriented along the fibre axial direction. The degree of crystallinity and crystallite size were both increased for the nanocomposite fibres and more significant for the fibres electrospun from 15% nanocomposite solution, which exhibited the finest average fibres size. As a result, the tensile properties of electrospun nanocomposites were greatly improved. The Young's modulus and ultimate strength of electrospun nanocomposite fibrous mats were improved up to 70% and 30%, respectively, when compared with PA-6 electrospun mats. However, the ultimate strength of the nanocomposite fibrous mats electrospun from 20% nanocomposites solution was decreased by about 20% due to their larger fibre sizes. The Young's modulus of PA-6 electrospun single fibres with a diameter around 80 nm was almost double the highest value that had been reported for the conventional PA-6 fibres and could be improved by about 100% for the electrospun nanocomposite single fibres of similar diameters.

Liang *et al.* [18] reported on a fibre that consisted of nano-Fe_2O_3 particles/PA-6 nanocomposite. The thermal stability of the composite material was enhanced about 16 °C (from 440 °C to 456 °C) by the addition of Fe_2O_3 nanoparticles with 15.0% content (part per hundred parts of resin). The Fe_2O_3 reinforced materials processed by melt spinning displayed improved tensile modulus compared to similarly processed pure PA-6, the improvements of tensile strength and

modulus were about 21% and 112%, respectively. Moreover, this fibre had the property of ultraviolet and visible light absorption.

In another interesting study [19], a range of polymer matrices were examined including polyvinyl alcohol, poly(9-vinyl carbazole) and polyamide. To compare production methods, polymer composite films and fibres were produced. It was found that by adding various mass fractions of nanofillers, both the Young's modulus and hardness increased significantly for both films and fibres. In addition, the thermal behaviour was seen to be strongly dependent on the nanofillers added to the polymer matrices. Wu *et al.* [20] prepared carbon fibre and glass fibre reinforced PA-6 and PA-6/clay nanocomposites. The fabrication method involved first mechanically mixing PA-6 and PA-6/clay with E-glass short fibre (6-mm long) and carbon fibre (6-mm long), separately. A twin-screw extruder at a rotational speed 20 rpm extruded the fibres. The temperature profiles of the barrel were 190–210–230–220°C from the hopper to the die. The extrudate was pelletized, dried, and injection moulded into standard test samples for mechanical properties test. The injection-moulding temperature and pressure were 230 °C and 13.5 MPa, respectively. The research found out that the tensile strength of PA-6/clay containing 30 wt.% glass fibres was 11% higher than that of PA-6 containing 30 wt.% glass fibre, while the tensile modulus of nanocomposite increased by 42%. Flexural strength and flexural modulus of neat PA-6/clay were found similar to PA-6 reinforced with 20 wt.% glass fibres. It was eluded that the effect of nanoscale clay on toughness was more significant than that of the fibre. Heat distortion temperatures of PA-6/clay and PA-6 were 112 °C and 62 °C, respectively. Consequently, the heat distortion temperature of fibre reinforced PA-6/clay system was almost 20°C higher than that of fibre reinforced PA-6 system. Notched Izod impact strength of the composites decreased with the addition of the fibre. The scanning electron microscopy (SEM) microphotographs showed that the wet-out of glass fibre was better than carbon fibre. The study concluded that the mechanical and thermal properties of the PA 6/clay nanocomposites were superior to those of PA-6 composite in terms of the heat distortion temperature, tensile and flexural strength and modulus without sacrificing their impact strength. This was attributed to the nanoscale effects, and the strong interaction force existed between the PA-6 matrix and the clay interface.

In case of short fibres, Akkapeddi [21] prepared PA 6-nanocomposites using chopped glass fibres. In a typical experiment, a commercial grade PA-6 of MW=30kg/mol and specially designed functional organo-quaternary ammonium-clay complexes (organoclays) based on MMT or hectorite type clays. Freshly dried PA-6 (moisture < 0.05%) was blended with 3-5 wt.% of a selected organoclay powder and extruded at 260 °C in a single step, under high shear mixing

conditions. Alternatively, the organoclay was master-batched first into PA-6 (at 25 wt. % loading and then re-extruded in a second step with more PA-6 to dilute the clay content to ≤ 5 wt.%. Conventional chopped glass fibre with 10 μm diameter and about 3 mm length was then added, as an optional reinforcement through a downstream feed port at zone 6 of the twin screw extruder. The glass fibre was compounded with the molten, premixed PA-6 nanocomposite either as a one-step extrusion process or in a second extrusion step. The extrudate was quenched in a water bath and pelletized. The pellets were dried under vacuum at 85 °C, and injection moulded into standard ASTM test specimens. As shown in Figure 1, significant improvements in modulus were achievable in both the dry and the moisture conditioned state for PA-6 nanocomposites compared to standard PA-6, at any given level of glass fibre reinforcement.

Figure 1

In particular, a small amount (3–4 wt.%) of nanometre scale dispersed layered silicate was capable of replacing up to 40 wt.% of a standard mineral filler or 10–15 wt.% of glass fibre to give equivalent stiffness at a lower density. In addition, improved moisture resistance, permeation barrier and fast crystallization/mould cycle time contribute to the usefulness of such composites.

Vlasveld *et al.* [22] developed three-phase thermoplastic composite, consisting of a main reinforcing phase of woven glass or carbon fibres and a PA-6 nanocomposite matrix. The nanocomposite used in this research had moduli that were much higher than unfilled PA-6, also above T_g and in moisture conditioned samples. Flexural tests on commercial PA-6 fibre composites showed decrease of the flexural strength upon increasing temperature. The researchers claimed that the strength of glass fibre composite can be increased by more than 40% at elevated temperatures and the temperature range at which a certain minimum strength is present can be increased by 40–50 °C. Carbon fibre composites also showed significant improvements at elevated temperatures, although not at room temperature. Based on flexural tests on PA-6 based glass and carbon fibre composites over a large temperature range up to near the melting point, it became clear that for these fibre composites it is important to have a reasonably high matrix modulus: Both glass and carbon composites were very sensitive to a decrease of the matrix modulus below values around 1 GPa. At higher moduli, carbon fibre composites are more sensitive to the matrix modulus than glass fibre composites. The modulus of unfilled PA-6 decreased below the (arbitrary) 1 GPa level just above T_g, it is noteworthy that the

nanocomposites used in this research had moduli that were much higher and stayed above the 1 GPa level up to 160 °C, which was more than 80 °C higher than for unfilled PA-6. The nanocomposites also showed much higher moduli in moisture conditioned samples, and even in moisture conditioned samples tested at 80 °C the modulus was much higher than that of the dry unfilled PA-6, again well above 1 GPa. DMA measurements showed that the nanocomposites did not show a change of T_g, and that the reduction of the modulus upon absorption of moisture was due to the T_g decrease.

In a parallel research, Vlasveld *et al.* [23] investigated fibre–matrix adhesion in glass-fibre reinforced PA-6 silicate nanocomposites. The main reinforcing phase consisted of continuous E-glass fibres, whereas the PA-6 based matrix was a nanocomposite reinforced with platelets of exfoliated layered silicate. Two different types of nanocomposite were used with different degrees of exfoliation of the silicate layers: one with non-modified silicate and one with an organically modified silicate. They developed nanocomposite laminates by sol–gel and modified diaphragm methods. The route for the preparation of PA-6 nanocomposites consisted of melt-compounding Akulon® K122D with Somasif® MEE and Somasif® ME-100 by means of a co-rotating twin-screw extruder at 240 °C. For the Somasif® MEE nanocomposite materials, first an 11 wt.% MEE master batch was compounded. To obtain the various concentrations of the MEE nanocomposite, the master batch was extruded for a second time without dilution for the 11 wt.% nanocomposite, or diluted with Akulon® K122D to concentrations of 6.1 and 2.7 wt.%. The 2.5 wt.% Somasif® ME-100 nanocomposite material was produced by diluting a 10% ME-100 master batch with Akulon® K122D in the extruder. (All mentioned percentages are weight percentages silicate as measured with a thermo-gravimetric analyser after heating for 40 min at 800 °C in air). Two demands for the preparation of the single fibre fragmentation specimens had to be met: the fibre had to lie straight in the centre of the specimen, and the matrix material of the specimen had to be thin enough to be transparent, since the fibre fragments were examined and measured using an optical microscope. A Fontijne hot plate press heated to 240 °C was used to produce the films necessary for the single fibre fragmentation test specimen preparation. Single fibres were carefully extracted from a fibre bundle and placed with a distance of approximately 2 cm parallel to each other between the PA or nanocomposite films. The hot plate press at the same temperature was used to melt the polymer films and a pressure of 0.8 N/mm^2 was applied for 30 s to provide the necessary bonding with the fibre. After cooling between cold metal plates, tensile test specimens were prepared. It was observed that the ultimate strength and stiffness increased by adding 1% SiO_2 nanoparticles, while little improvement in fatigue behaviour was

found. It was conclude that the failure mechanism was by interfacial de-bonding and that both the addition of nanoparticles and moisture conditioning had a negative effect on the bonding between the matrix and the glass fibres. In addition, the researchers noted that in the formed composites the adhesion between the nanocomposites and the carbon fibres (Figure 2) was probably worse than between the unfilled PA-6 and the matrix, reducing the potentially positive influence of the increased matrix modulus.

Figure 2

An assessment of reactively processed anionic polyamide-6 (APA-6) for use as matrix material in fibre composites was conducted by van Rijswijk *et al.* [24] and they also compared it with melt processed PA-6 and PA-6 nanocomposites. A special designed lab-scale mixing unit was used to prepare two liquid material formulations at 110 °C under a nitrogen atmosphere: a monomer/activator-mixture in tank A and a monomer/initiator-mixture in tank B, as shown on Figure 3.

Figure 3

After individually degassing both tanks (15 min at 100 mbar), the two material feeds were mixed by using a heated (110 °C) static mixer and dispensed (1:1 ratio) into a heated (110 °C) buffer vessel with nitrogen protective environment. Stainless steel infusion mould (Figure 3), was used together with a 3 mm thick stainless steel cover plate (not shown) to manufacture neat APA-6 panels (250×250×2 mm). Homogeneous heating of the mould was obtained by placing it in a vertically positioned hot flat platen press. A silicon tube connected the resin inlet of the mould with the buffer vessel and the resin outlet with a vacuum pump. Infusion from bottom to top was necessary to prevent entrapment of air. A pressure control system was used to precisely set the infusion and curing pressure (absolute pressure in the mould cavity). Loss of control over the pressure in the mould cavity due to solidification of resin in the unheated outlet tube had to be prevented. To avoid this, a buffer cavity was machined in the mould near the outlet to slow down the infusion, hence giving ample time to stop the resin flow before it was able to exit the mould. For every infusion pressure, the infusion time to reach the buffer cavity was determined visually by replacing the steel cover plate by a glass one. Additionally, a resin trap and a cold trap were placed directly after the mould to protect the vacuum pump. The mechanical properties of APA-6

and HPA-6 (Akulon® K222D, low MW injection-moulding grade hydrolytically polymerised PA-6) nanocomposites were compared with injection moulded neat HPA-6. As expected, the HPA-6 nanocomposite had the highest modulus over the entire range of temperatures (20–160 °C) and moisture contents (0–10 wt.%) tested. However, APA-6 came close and had the highest maximum strength due to its characteristic crystal morphology, which was directly linked to the reactive type of processing used. This same morphology, it was claimed, also made APA-6 slightly less ductile compared to melt processed HPA-6. Compared to the melt processed HPA-6, APA-6 polymerised at 150 °C and the HPA-6 nanocomposite offered a higher modulus at similar temperature, or similar modulus at a higher temperature (40–80 °C increase). It is noteworthy that such an increase in maximum use temperature, related to the heat distortion temperature, can seriously expand the application field of PA-6 and PA-6 composites. For all PAs, temperature and moisture absorption reduced the modulus and the strength and increased the maximum strain, which was directly related to the glass transition temperature. Whereas with increasing testing temperature at a certain moment the T_g of the dry polymer was exceeded, moisture absorption reduced the T_g at a certain point below the testing temperature. However, the effect of both was in essence the same. Retention of mechanical properties of APA-6 after conditioning at 70 °C for 500 h and subsequent drying was demonstrated. Conditioning submersed in water at the same temperature, however, resulted in a brittle material with surface cracks, as is common to most polyamides. Continued crystallization and removal of unreacted monomer caused this behaviour. Given the fact that submersion at elevated temperatures is usually not an environment in which PA-6 and its composites are applied, the encountered property reduction was therefore not detrimental for application of these materials. The overall conclusion of the comparative study for application of the polyamides as matrix material in fibre composites was that both APA-6 and the HPA-6 nanocomposites outperformed the melt processed HPA-6 in terms of modulus and maximum strength. Therefore, the researchers concluded that both “improved” PAs may be expected to enhance the matrix dominated composite properties like compressive and flexural strength, provided that a strong fibre-to-matrix interphase is obtained.

Another comparative study was conducted by Sandler *et al.* [25] on melt spun PA-12 fibres reinforced with carbon nanotubes and nanofibres. A range of MWNT and carbon nanofibres were mixed with a PA-12 matrix using a twin-screw microextruder, and the resulting blends spun to produce a series of reinforced polymer fibres. The work aimed to compare the dispersion and resulting mechanical properties achieved for nanotubes produced by the electric arc and a variety of chemical vapour deposition techniques. A high quality of dispersion was achieved for all the

catalytically-grown materials and the greatest improvements in stiffness were observed using aligned, substrate-grown, carbon nanotubes. The use of entangled MWNT led to the most pronounced increase in yield stress, most likely as result of increased constraint of the polymer matrix due to their relatively high surface area. The degrees of polymer and nanofiller alignment and the morphology of the polymer matrix were assessed using X-ray diffraction (XRD) and differential scanning calorimetry (DSC). The carbon nanotubes were found to act as nucleation sites under slow cooling conditions, the effect scaling with effective surface area. Nevertheless, no significant variations in polymer morphology as a function of nanoscale filler type and loading fraction were observed under the melt spinning conditions applied. A simple rule-of-mixture evaluation of the nanocomposite stiffness revealed a higher effective modulus for the MWNT compared to the carbon nanofibres, as a result of improved graphitic crystallinity. In addition, this approach allowed a general comparison of the effective nanotube modulus with those of nanoclays as well as common short glass and carbon fibre fillers in melt-blended PA composites. The experimental results further highlighted the fact that the intrinsic crystalline qualities, as well as the straightness of the embedded nanotubes, were significant factors influencing the reinforcement capability.

2.2 Polyesters nanocomposites

Jawahar and Balasubramanian [26] prepared glass fiber reinforced polyester composite and hybrid nanoclay-fibre reinforced composites by hand lay-up process. The composites were prepared with a glass fibre content of 25 vol.% and the proportion of the nanosize clay platelets was varied from 0.5-2.5 vol.%. The investigation found out that the hybrid clay-fibre reinforced polyester composite possed better tensile, flexural, impact, and barrier properties, better shear strength, storage modulus, and glass transition temperature. The optimum properties were found to be with the hybrid laminates containing 1.5 vol.% nanosize clay. Also, Chandradass *et. al.* [27] successfully fabricated vinyl ester glass fibre reinforced composites filled individually with organic clay at room temperature using hand lay up technique. The hybrid composites were fabricated in two steps: in the first step organoclay was mixed with vinyl ester resin and the second step was the hand lay-up process of making composites of 4 layers of chopped strand mat (CSM). The four layers of CSM glass fibre mats were cut in the size of 35 cm × 35 cm. These were weighed to take the corresponding 1:1 amount of epoxy resin. The organoclay dry particles with several percentages by weight of clay (1, 3, and 5%) were mixed with the vinyl ester resin at

the room temperature. Appropriate amount of the organomodified clay was added to the resin and mechanically stirred by "high shear" mixture at 1000 rpm for 1 h. The degassing of the mixture was done for 1 h. The resin–clay premixed mixture resulted in well-dispersed, stable suspension of the clay in the vinyl ester resin. 2 wt.% of methyl ethyl ketone peroxide (MEKP) as catalyst, benzoyl peroxide as promoter and cobalt napthalate as accelerator was then added to the pre-mixed clay in vinyl ester resin at room temperature to initiate the cross-linking process. Then, this resin–clay mixture was used to fabricate the 4 layers of E-glass CSM in the hand lay-up technique. Samples are allowed to cure for 24 h at room temperature. Mechanical testing revealed improved natural frequency and damping factor in organic clay filled hybrids over vinyl ester glass fibre reinforced composites. Natural frequency increases in organically modified clay filled hybrids for clay up to 3 wt.%, and on further increase, natural frequency decreases. At high content (> 3%), the agglomeration, weak fibre–matrix interface dominated in the matrix caused low stiffness.

2.3 Polyurethane (PU) nanocomposites

Poulin [28, 29] used conductive complex of polyaniline and sulfonated urethane to blend two forms of CNT into thermoplastic elastomeric PU for processing into nanotube-containing nanofibres. The polyelectrolyte was presumed to provide the ionic doping of the templated PANI in the complex and assisted in plasma-enhanced CVD prepared CNT (1-5 μm long and straight), and furnace CVD prepared CNT (5-10 μm long, coiled and twisted). Elsewhere, composite nanofibres and films have been made from the homogeneous SWNTs/PU dispersions by solution mixing [30, 31]. More recently, Chen *et al.* [32] reported the fabrication and mechanical studies of CNT/PU composite fibres by melt-extrusion process, in which chemically functionalized MWNT were used. Good dispersion in PU with MWNT at significant weight fraction and greatly improved overall mechanical properties were achieved. Mechanical tests showed that, compared with pure TPU, the tensile modulus, tensile strength were improved significantly while without sacrificing high elongation at break by incorporating MWNT less than ~9.3 wt.%. Homogeneous dispersion of MWNT throughout PU matrix and the strong interfacial adhesion between functionalized MWNT and the matrix were proposed to be responsible for the significant mechanical enhancement. They reported unusual combination of increased tensile strength and Young's modulus without sacrificing high elongation at break which is prominently important for the PU development. In addition, ultra fine elastic fibres with submicron diameters were

successfully produced by electrospinning of PU-urea (PUU) solutions [33]. A two-step procedure was followed during the preparation of segmented PUU copolymers. The first step was the formation of isocyanate-terminated prepolymer, followed by the addition of dibutylamine to control the molecular weight (aimed at 25 000 Da). The second step was the chain extension with 2-methyl-1,5-diaminopentane to form high molecular weight copolymers. Fibre diameters in the range 7 nm to 1.5 μm were obtained by varying the solution concentration. The fibre diameters increased as the third power of solution concentration. The highest polymer concentration which could be electrospun into fibres was 13 wt.% at room temperature, whereas the concentration done at the high temperature was 21 wt.%. Viscosity of the solution was determined as the dominant factor among the other solution properties. However, the study did not compare the viscosity values of the two concentration solutions, which were electrospun at two different temperatures. One important finding of the study was that while electrospinning PU nanofibres, the researchers found out that the fibre diameters obtained from the polymer solution at a high temperature (70 ºC) were much more uniform than those at room temperature. Although the mechanisms involved were not fully understood, the study was a useful step towards obtaining uniform nanofibres which is one of the current challenges facing electrospinning nanofibres production.

2.4 Polypropylene (PP) nanocomposities

Low-cost commodity resins such as polypropylene (PP), suffer primarily due to low compressive strength. Generally, enhancement of the compressive strength of pultruded thermoplastic composites is achieved by improving the yield strength of the surrounding matrix in shear and reducing fibre misalignment in the composite through optimization of manufacturing process variables. The dispersed platelets are typically one micron in length but only a nanometer in thickness. Roy *et al.* [34] studied the compressive strength of pultruded PP thermoplastic composites using nanoclay reinforcement. A single-screw extruder was used to facilitate nanoclay dispersion in PP. After the prepreg was pultruded to form a composite laminate, uniaxial compression tests were performed to determine compression strength of the laminate. This new family of materials exhibited enhanced stiffness and strength of the matrix material, through the inclusion of exfoliated nano-stale montmorillonite particles in the fabrication of resin pre-impregnated (prepreg) glass fibre filaments. The study observed consistent improvement in the compressive strength and modulus up to about 122% at 10% clay loading. Kumar *et. al.* [35]

demonstrated that fibres from PP/nano carbon fibre composites can be spun using the conventional melt spinning equipment and possess superior modulus and compressive strength at 5 wt.% loading of nano carbon fibre. Scanning electron microscopy revealed a good dispersion of the nano carbon fibre by melt processing in PP matrix. While the observed fibre moduli had improved significantly (50%) by reinforcement with the nano carbon fibres, rule of mixtures calculations suggested that further improvements in modulus were likely, if perfect alignment and perhaps better interfacial adhesion of nano carbon fibres could be achieved in the polypropylene matrix fibre. In the meantime, Zhang *et al.* [36] investigated thermal degradation of fibre forming PP containing dispersed nanoclays. The work concluded that the dispersion of Bentone 107 clay can be greatly improved by the addition of grafted-PP. Some degree of exfoliation could be achieved for the sample-containing diethyl-*p*-vinylbenzyl phosphonate (DEpVBP) grafte-PP. The fire performance of PP was effectively improved by the addition of nanoclay in conjunction with conventional phosphorus flame retardant and phosphorus containing grafting monomers. The researchers lamented that a better dispersion of nanoclay in the composite did not necessarily increase its fire performance due to the negative effect to the degradation caused by the addition of grafting monomers. However, further investigations are required for a better understanding of the degradation mechanism of the fibre-reinforced nanocomposites with improved fire performance.

2.5 Poly(ethylene) nanocomposites

Raun *et al.* [37] reported on the use of CNT in a highly oriented polymer matrix to investigate toughening effects in the homopolymer. By incorporating 1 wt.% MWNTs into highly oriented ultra-high molecular weight poly(ethylene) (UHMWPE) films, a 150% increase in strain energy absorption before failure under tensile loading and a 25% increase in tensile strength was achieved. Micro-Raman spectroscopy of the nanofibre under loading showed the multi-scale interactions between the highly aligned UHMWPE molecules and the embedded MWNT. It was also observed that at intermediate strains, the MWNTs acted as slippage sites, allowing the matrix to deform without significant bond stretching. However, these sites acted as pseudo taut tie molecules at large strains to produce the strain hardening effects that were absent from the highly anisotropic pure UHMWPE films. In a recent work, Raun and co-workers [38] demonstrated that adding MWNTs can lead to super strong and ductile UHMWPE composite fibres. A simultaneous toughening and strengthening effect was observed in these composite

fibres. The 5 wt.% MWNT/UHMWPE composite fibres showed the highest specific tensile strength and energy to fracture amongst all commercial high performance fibres. The researchers predicted that these properties would make gel-spun UHMWPE even more competitive in the area of high-energy absorption applications such as in ballistic vests. The strong interfacial interaction between the dispersed MWNT and the matrix PE was demonstrated through DSC, SEM and micro-Raman spectroscopy. The CNT acted as nucleating sites for PE crystal growth. In situ CNT orientation along the fibre direction occurred through CNT pulling out from the micron-sized CNT dominated clusters at high draw ratios. The elongated CNT were dispersed as individual tubes or bundles of a few CNTsintimately surrounded by the UHMWPE matrix. Raman spectroscopy confirmed that such conformations of CNT reinforced the UHMWPE matrix both in terms of stiffness and tensile strength. The stiffness was enhanced through load bearing effect at small strains while the tensile strength was enhanced by strain hardening effect on the matrix. The tensile modulus and strength of the composite fibre appeared to show very good agreement with the predictions of the rule of mixtures. As not all the CNT were aligned with the matrix PE, it was suspected that further alignment or better dispersion of CNT may lead to more positive deviations from the rule of mixtures. In another work, compatibilized and noncompatibilized polymer blends based on high-density polyethylene (PE) and PA-12 or PA-6 taken in various proportions were prepared by consecutive melt blending, extruding, and cold drawing [39]. These blends were, afterward, subjected to compression moulding to obtain the microfibrillar-reinforced materials in which isotropic and relaxed PE matrixes were reinforced by differently oriented PA fibrils. The orientation of the latter was studied by means of two-dimensional SAXS in a synchrotron as a function of the blends' chemical compositions and compatibilizations. Based on the analysis of the SAXS patterns, a model was proposed, explaining the role of the PA type and polyethylene-co-maleic anhydride compatibilizer in the orientation of the PE-PA precursors and composites during the various stages of preparation.

2.6 Other examples of fibre-reinforced nancomposites

Ji *et al.* [40] characterized the surface nanomechanical properties of electrospun polystyrene (PS) fibres by shear modulation force microscopy (SMFM) and found that the relative surface modulus of electrospun PS single fibres increased with the decreasing fibre sizes. Qian *et al* [41] conducted an experimental study and showed that the addition of 1 wt.% CNT resulted in a 36–42% increase in the elastic stiffness and a 25% increase in the tensile strength for polystyrene

(PS)-based composites. Liao and Li [17] performed molecular mechanics simulations and elasticity calculations to predict the interfacial characteristics of a CNT–PS composite system. They simulated the pull-out of CNT from the matrix and calculated the CNT–PS interfacial shear strength to be around 160 MPa.

Dror and Zussman [42] fabricated electrospun nanocomposite fibers of poly(ethylene oxide) (PEO), in which MWNT were embedded. They found that PEO crystals were highly aligned along the fibre axis during the electrospinning process. The MWNT were embedded in the nanofibres as individual elements, mostly aligned along the fibre axis. Zeng *et. al.* [43] prepared poly(ethylene terephthalate) (PET)-based composite fibres by melt spinning three types of PET/polyhedral oligomeric silsesquioxane (POSS) composites. These composites were made by either melt blending POSS with PET at 5 wt.% loading level (non-reactive POSS and silanol POSS) or by in-situ polymerization with 2.5 wt.% reactive POSS. Significant increases in tensile modulus and tensile strengths were achieved in PET fibres with non-reactive POSS at room temperature. The high temperature modulus retention was found to be much better for PET/silanol POSS fibre when compared to that of control PET. Although other PET/POSS nanocomposite fibres tested did not show this high retention of modulus at elevated temperatures, PET/isooctylPOSS nanocomposite fibres did show increased modulus at elevated temperature compared to that of PET. Higher compressive strengths, compared to PET fibres, were observed for all three nanocomposite fibres. Gel permeation chromatography measurement suggested that there was no significant change in molecular weight during preparation of PET/POSS nanocomposites. SEM observations suggested that there was no obvious phase separation in any of the three PET/POSS systems. Crystallization behaviour and thermal stability of the composite were also studied. The fibre spinning and mechanical performance with 10 and 20 wt.% of trisilanolisooctyl POSS were also investigated. It was noted that the nanocomposites with higher concentrations of this nanofiller can be spun without any difficulty. At room temperature, the fibre tensile modulus increased steadily with the POSS concentration while fibre tensile strength showed no significant change. The elongation at break decreased significantly with increasing of POSS concentration. The high-temperature moduli of PET/POSS nanocomposite fibres were found to be rather variable, likely due to the modest compatibility between filler and polymers, which lead to structural anisotropy within the composite.

3. High performance/temperature fibre-reinforced nanocomposites

3.1 Poly(ether ether ketone) (PEEK)

Jen *et al.* [44] manufactured AS-4/PEEK APC-2 nano-composite laminates and also studied their mechanical responses. The experimental procedure were as follows: firstly, the nanoparticles were diluted in alcohol (50 ml alcohol:2 g SiO_2) and stirred uniformly, then 16 plies of $[0/90]_{4s}$ cross-ply and $[0/\pm45/90]_{2s}$ quasi-isotropic prepregs were cut, SiO_2 solution was then spread on the prepreg in a temperature-controlled box, and later weighed the nanoparticles after evaporation of alcohol in the range of 111–148 mg/ply. A repeat on spreading for 5, 8, 10, 15 plies, was the next step followed by curing (the curing process is shown in Figure 4) the stacked plies in a hot press to form a laminate of 2 mm thick.

Figure 4

Next, the laminates were cut into specimens and tested according to ASTM D3039M. The tensile tests were repeated at 50, 75, 100, 125, 150 °C to receive respective stress–strain curve, strength and stiffness, and the obtained data compared with the original APC-2 laminate (no SiO_2 nanoparticles) to find the optimal SiO_2 % by weight. From tensile tests it was found out that the optimal content of nanoparticles (SiO_2) was 1% by total weight. The ultimate strength increased by about 12.48 % and elastic modulus 19.93 % in quasi-isotropic nano-laminates, whilst, the improvement of cross-ply nano-composite laminates was less than that of quasi-isotropic laminates. At elevated temperatures the ultimate strength decreased slightly below 75 °C and the elastic modulus reduced slightly below 125 °C, however, both properties degraded highly at 150 °C ($\approx T_g$) for the two lay-ups. Finally, after the constant stress amplitude tension–tension (T–T) cyclic testing, it was found that both the stress-cycles (S–N) curves were very close below 10^4 cycles for cross-ply laminates with or without nanoparticles, and the S–N curve of nano-laminates slightly bent down after 10^5 cycles.

Sandler *et al.* [45] produced poly(ether ether ketone) nanocomposites containing vapour-grown carbon nanofibres (CNF) using standard polymer processing techniques. Macroscopic PEEK nanocomposite master batches containing up to 15 wt.% vapour grown CNF were prepared using a Berstorff co-rotating twin-screw extruder with a length-to-diameter ratio of 33. The processing temperatures were set to about 380 °C. The strand leaving the extruder was quenched in a water bath, air dried and then regranulated followed by drying at 150 °C for 4 h. Tensile bars according

to the ISO 179A standard were manufactured on an Arburg Allrounder 420 injection moulding machine at processing temperatures of 390 °C, with the mould temperature set to 150 °C. Prior to mechanical testing, all samples were heat treated at 200 °C for 30 min followed by 4 h at 220 °C in an attempt to ensure a similar degree of crystallinity of the polymer–matrix. Macroscopic tensile tests were performed at room temperature with a Zwick universal testing machine. The cross-head speed was set to 0.5 mm/min in the 0–0.25% strain range and was then increased to 10 mm/min until specimen fracture occurred. Evaluation of the mechanical composite properties revealed a linear increase in tensile stiffness and strength with nanofibre loading fractions up to 15 wt.% while matrix ductility was maintained up to 10 wt.%. Electron microscopy confirmed the homogeneous dispersion and alignment of nanofibres. An interpretation of the composite performance by short-fibre theory resulted in rather low intrinsic stiffness properties of the vapour-grown carbon nanofibre. Differential scanning calorimetry (DSC) showed that an interaction between matrix and the nanoscale filler could occur during processing. However, such changes in polymer morphology due to the presence of nanoscale filler need to be considered when evaluating the mechanical properties of such nanocomposites.

Schmidt [46] investigation involved multifunctional inorganic-organic composite sol-gel coatings for glass surfaces. The sol-gel process allowed the fabrication of ceramic colloidal particles in the presence of organo alkoxy silanes carrying various functions and the synthesis of multi-functional transparent inorganic-organic composites. The report claimed that in addition, these composites can be used as controlled release systems or designed as gradient systems. Using this approach, a coating with a very low surface free energy (antisoiling properties) and temperature stability up to 350 °C, a controlled release system for permanent wettability (anti-fogging) and systems containing metal colloids for optical effects were developed. Lin [47] and Wang *et al.* [48] studied the effect on wear and friction by adding SiC nanoparticles in PEEK. The latter studied the effect of the synergism between nanometer SiC and PTFE on the wear of PEEK. The PEEK fine powders (ICI grade 450P, η=0.62) in a diameter of approximately 100 μm, were prepared. The nanometer SiC used as filler had the size smaller than 80 nm. The PTFE powders (diameter 25 μm), nanometer SiC and PEEK were fully mixed ultrasonically, dispersed in alcohol for ~15 min. Then the mixture was dried at 110 °C for 6 h to remove the alcohol and moisture. Finally, the mixture was moulded into the block specimens by compression moulding, in which the mixture was heated at a rate of 10 °C min^{-1} to 340 °C, held there for 8 min, and then cooled in the mould to 100 °C. After releasing from the mould, the resultant block specimen was prepared for friction and wear tests. A tribological study found that the incorporation of PTFE

into 3.3 vol.% nanometer SiC filled PEEK had a detrimental effect on the tribological properties of SiC–PTFE–PEEK composite. The morphologies of worn surfaces and the properties of transfer films deteriorated, while the load-carrying capacity of the SiC–PTFE–PEEK composite was also adversely affected. The researchers claimed the reason for this was due to SiF_x, which was formed on the original surface and worn surface during the compression moulding process and sliding friction process, as a result of the chemical reaction between nanometer SiC and PTFE. The chemical reaction and the formation of SiF_x dominated the tribological behaviour of the SiC–PTFE–PEEK composites filled with various contents of PTFE and 3.3 vol.% nanometer SiC. When the PTFE volume percentage was low then the SiF_x caused the friction and wear of the SiC–PTFE–PEEK composite to rise. However, at high volume percents the low friction PTFE dominated the friction and wear behaviours and the friction decreased as the percentage of PTFE increased. The chemical reaction and the formation of SiF_x led to changes in the worn surface morphologies and detrimental effect on the characteristics of the transfer films.

3.2 Polyimide nanocomposites

Ogasawara *et al.* [49] directed their investigations toward improvement of heat resistance of a relatively new phenylethynyl terminated imide oligomer (Tri-A PI) by loading of MWNT. They fabricated the MWNT/Tri-A PI composites containing 0, 3.3, 7.7, and 14.3 wt.% MWNT using a mechanical blender without any solution (dry condition) for several minutes. The volume fraction of MWNT were calculated to be 2.3, 5.4, 10.3 vol.% from the density of the MWNT (1.9 g/cm^3) and the cured polyimide (1.3 g/cm^3). Scanning electron micrographs showed the particle size of the imide oligomers to be in the range of 0.1–10 μm, and MWNT were not dispersed uniformly in the mixture. The loss of aspect ratio during the mechanical blending was not significant; therefore the MWNT were flexible for mechanical blend process with the imide oligomers. The preparation of the nanocomposite involved the melt mixing of MWNT/imide oligomer at 320 °C for 10 min on a steel plate in a hot press, and then curing at 370 °C for 1 h under 0.2 MPa of pressure with PTFE spacer (thickness 1 mm). The resulting composites containing 3.3, 7.7, 14.3 wt.% MWNT exhibited relatively good dispersion in macroscopic scale. Tensile tests on the composites showed an increase in the elastic modulus and the yield strength, and decrease in the failure strain. Figure 5 shows the effect of the MWNT concentration on Young's modulus of the composites.

Figure 5

Dynamic mechanical analysis (DMA) showed an increase in the glass transition temperature with incorporation of the carbon nanotubes. The experimental results suggested that the carbon nanotubes were acting as macroscopic crosslinks, and were further immobilizing the polyimide chains at elevated temperature. As to the reason why dispersed MWNT increased the heat distortion temperature the researchers explained that the dispersed MWNT impedes the molecular motion in polyimide network at elevated temperature. The other property improvements in this material are that MWNT showed some potential for controlling electric conductivity and electro-magnetic wave absorbability. Although static properties were obtained, discussions were not given, and it is evident that more research work would be required to prove that the suggested phenomenon is a true cause of higher glass transition temperatures.

3.3 Polyarylacetylene (PAA) nanocomposites

Polyarylacetylene (PAA) is going through increasing development in the field of advanced heat resistant composites owing to its outstanding heat resistance and excellent ablative properties. Fu *et al.* [50] have reviewed the advantages of PAA resin over the state-of-the-art heat resistant resin. The main potential applications of PAA resin are used in conventional resin matrix composites with ultra-low moisture outgassing characteristics and improved dimensional stability suitable for spacecraft structures, as an ablative insulator for solid rocket motors, and as a precursor for carbon–carbon composites. Carbon fibre reinforced PAA composites (carbon fibre/PAA) undoubtedly play a very important role in all these fields. Unfortunately, the mechanical properties of the carbon fibre/PAA material are not yet sufficiently satisfactory to replace the widely used heat resistant composites such as carbon or graphite reinforced phenolic resin. The mechanical properties of carbon fibre reinforced resin matrix composites depend on the properties of carbon fibre and matrix, especially on the effectiveness of the interfacial adhesion between carbon fibre and matrix.

PAA has high content of benzene ring and hence a highly cross-linked network structure, which render the material brittle. Moreover, the chemical inert characteristics of the carbon fibre surface lead to weak interfacial adhesion between fibres and non-polar PAA resin. To ensure that the material could be used safely in complicated environmental conditions and to exploit the excellent heat resistant and ablative properties more effectively, it is necessary to improve the

mechanical properties of the carbon fibre/PAA composites. To achieve this purpose, two kinds of methods can be used. One method is to improve the properties of PAA resin by structural modification or by intermixing other resins, such as phenolic resin. The other is treatment of carbon fibre surface. The treatment of carbon fibre surface has been studied for a long time and several methods such as heat treatment, wet chemical or electrochemical oxidation, plasma treatment, gas-phase oxidation, and high-energy radiation technique have been demonstrated to be effective in the modification of the mechanical interfacial properties of composites based on polar resins such as epoxy. In Zang *et al*. [51] investigations, for instance, carbon fibres were treated with oxidation–reduction followed by vinyltrimethoxysilanes-silsesquioxane (VMS–SSO) coating method to improve the interfacial mechanical properties of the carbon fibre/PAA composites. The carbon fibre surface treatment process is shown in Figure 6.

Figure 6

Polar functional groups, including carboxyl and hydroxyl, on carbon fibre surface were imported after the oxygen plasma oxidation treatment. The quantity of carboxyl on carbon fibre surface was decreased and that of hydroxyl on carbon fibre surface was increased after the $LiAlH_4$ reduction treatment. The $LiAlH_4$ reduction time was decided according to the experimental parameter of Lin [52]. The VMS–SSO coating was grafted onto the carbon fibre surface by the reaction of the hydroxyl in VMS–SSO and that on carbon fibre surface. The VMS–SSO coating concentrations and treatment time were decided according to Zhang *et al.* [53] who had optimized VMS–SSO coating treatment parameters. The investigation found out that interlaminar shear strength of the carbon fibre/PAA composites was increased by 59.3% at the end of treatment [51]. The conclusion that carbon fibre surface oxidation–reduction followed by silsesquioxane coating treatment is an effective method to improve the interfacial mechanical properties of carbon fibre/PAA composites were drawn. This kind of method could be widely used in different resin matrix composites by changing the functional groups on silsesquioxanes according to that on the resin.

3.4 Poly(p-phenylene benzbisoxazole) (PBO) fibre reinforced nanocomposites

Poly(p-phenylene benzbisoxazole) (PBO), a rigid-rod polymer, is characterized by high tensile strength, high stiffness, and high thermal stability. Kumar *et al.* [54] found out that PBO/CNT

reinforced fibres exhibited twice the energy absorbing capability than the plain PBO fibres. The nanocomposites were prepared as follows: into a 250 mL glass flask, equipped with a mechanical stirrer and a nitrogen inlet/outlet, were placed ~4.3 g (0.02 mol) of 1,4-diaminoresorcinol dihydrochloride, ~4 g (0.02 mol) of terephthaloyl chloride, and ~12 g of phosphoric acid (85%). The resulting mixture was dehydrochlorinated under a nitrogen atmosphere at 65 °C for 16 h and subsequently at 80 °C for 4 h. At this stage, 0.234 g of purified and vacuum-dried HiPco nanotubes was added to the reaction flask. The mixture was heated to 100 °C for 16 h while stirring and then cooled to room temperature. P_2O_5 (8.04 g) was added to the mixture to generate poly(phosphoric acid) (77% P_2O_5). The mixture was stirred for 2 h at 80 °C and then cooled to room temperature. Further P_2O_5 (7.15 g) was then added to the mixture to bring the P_2O_5 concentration to 83% and the polymer concentration to 14 wt.%. The mixture was heated at 160 °C for 16 h with constant stirring. Stir opalescence was observed during this step. The mixture was finally heated to 190 °C for an additional 4 h while stirring. An aliquot of the polymer solution was precipitated, washed in water, and dried under vacuum at 100 °C for 24 h. An intrinsic viscosity of 14 dL/g was determined in methanesulfonic acid at 30 °C. A control polymerization of pure PBO was also carried out under the same conditions without adding SWNT. For PBO/SWNT (90/10) composition, 0.47 g of purified HiPco tubes (SWNT) was added to the mixture. The sequence of steps and polymerization conditions remained the same as those for PBO/SWNT (95/5) composition. Intrinsic viscosity values of PBO and PBO/SWNT (90/10) were 12 and 14 dL/g, respectively. Single-walled nanotubes were well dispersed during PBO synthesis in PPA. PBO/SWNT composite fibres were successfully spun from the liquid crystalline solutions using dry-jet wet spinning. The addition of 10 wt.% SWNT increased PBO fibre tensile strength by about 50% and reduced shrinkage and high-temperature creep. The existence of SWNT in the spun PBO/SWNT fibres was evidenced by the 1590 cm^{-1} Raman peak.

4. Conclusions

So far, most of the scientific work has been focussing on the synthesis of polymer nanocomposites and on the study of their physical and mechanical properties. The use of these nanocomposites as matrix in fibre-reinforced composites is in its infancy. Nano-composites from polymeric matrix materials (thermoplasts or thermosets) reinforced with nano-sized fillers such as carbon nano-tubes, nano-sized particles or intercalated layers are an active area of research. This is macroscopically depicted in the increase in for instance, fracture energy values. Similar

effects have been reported for nanoparticles reinforcement. Nanofillers, due to their size, can be significantly present in this small zone while in the case of micro-particles only few of them participate in the plastic zone deformation. In this way, nanofillers can lead to increased fracture properties of the brittle matrix. On the other hand, the matrix material is pointed out to be a key parameter for the mode I delamination resistance of fibre reinforced polymers. Therefore, enhancement in the matrix fracture toughness can lead to an overall advanced fracture behaviour. Additionally, the influence of the nanofibers has also been extended to the reinforcing fibres by making mores nanofibres to be involved during the delamination process and thus increasing the fracture toughness.

A key advantage of the use of nanocomposite instead of other polymers to improve the fibre composite properties is that the properties can be improved without any change in the processing conditions. The most promising current approaches towards increasing the orientation of nanoscale reinforcements within a matrix include optimisation of the extrusion die and stretching the composite melt to form films and fibres. One complication is that the microstructure of semicrystalline polymer matrices is influenced not only by the processing history but also by the presence of nanoparticles. The addition of various types of carbon nanotubes and nanofibres to polymers has already been observed to influence the crystallisation kinetics and resulting morphology. Such changes in matrix morphology need to be considered when evaluating the nanocomposite performance with regard to the intrinsic filler properties. The effects of carbon nanotubes or nanofibres on such oriented polymer systems, although significant, have not yet been fully established. Finally, it should be noted that the presence of additives such as colouring pigments has been shown to influence matrix morphology during fibre spinning, whilst there is the whole technology of nucleating agents which are deliberately added to influence crystalline microstructure. Nanoparticle reinforcement of fibre reinforced composites has been shown to be a possibility, but much work remains to be performed in order to understand how nanoreinforcement results in major changes in material properties. The understanding of these phenomena will facilitate their extension to the reinforcement of more complicated anisotropic structures and advanced polymeric composite systems. The property and performance enhancements made possible by nanoparticle reinforcement may be of great utility for fibre-reinforced composites.

5. References

[1] Sinha RS, Okamoto M. Polymer/layered silicate nanocomposites: A review from preparation to processing. *Prog. Polym. Sci.* 2003; **28:** 1539-1641.

[2] Kornmann X, Lindberg H, Berglund LA. Synthesis of epoxy–clay nanocomposites: influence of the nature of the clay on structure. *Polymer.* 2001; **42:** 1303-1310.

[3] Zilg C, Thomann R, Finter J, Mulhaupt R. The influence of silicate modification and compatibilizers on mechanical properties and morphology of anhydride-cured epoxy nanocomposites. *Macromol. Mater. Eng.* 2000; **280-281:** 41-46.

[4] Kashiwagi T, Grulke E, Hilding J, Harris R, Awad W, Douglas J. Thermal degradation and flammability properties of poly(propylene)/carbon nanotube composites. *Macromol. Rapid Comms.* 2002; **23:** 761-765.

[5] Njuguna J, Pielichowski K. Polymer nanocomposites for aerospace applications: fabrication. *Adv. Eng. Mater.* 2004; **6:** 193-203.

[6] Njuguna J, Pielichowski K. Polymer nanocomposites for aerospace applications: Characterization. *Adv. Eng. Mater.* 2004; **6:** 204-210.

[7] Andrews R, Jacques D, Minot M, Rantell T. Fabrication of carbon multiwall nanotube/polymer composites by shear mixing. *Macromol. Mater. Eng.* 2002; **287:** 395-403.

[8] Njuguna J, Pielichowski K. Polymer nanocomposites for aerospace applications: properties. *Adv. Eng. Mater.* 2003; **5:** 769-778.

[9] Pinnavaia TJ, Lan T, Wang Z, Shi H, Kaviratna PD. Clay-Reinforced Epoxy Nanocomposites: Synthesis, Properties, and Mechanism of Formation. *ACS Symposium Series.* 1996; **622:** 250-261.

[10] Leszczyńska A, Njuguna J, Pielichowski K, Banerjee JR. Polymer/montmorillonite nanocomposites with improved thermal properties: Part II. Thermal stability of montmorillonite nanocomposites based on different polymeric matrixes. *Therm. Acta.* 2007; **454:** 1-22.

[11] Leszczyńska A, Njuguna J, Pielichowski K, Banerjee JR. Polymer/montmorillonite nanocomposites with improved thermal properties: Part I. Factors influencing thermal stability and mechanisms of thermal stability improvement. *Therm. Acta.* 2007; **453:** 75-96.

[12] Liu T, Ping Lim K, Chauhari Tjiu W, Pramoda KP, Chen Z. Preparation and characterization of nylon 11/organoclay nanocomposites. *Polymer.* 2003; **44:** 3529-3535.

[13] Usuki A, Kawasumi M, Kojima Y, Okada A. Swelling behavior of montmorillonite cation exchanged for ω-amino acids by ε-caprolactam, *J. Mater. Res.* 1993; **8:** 1174-1178.

[14] Lincoln DM, Vaia RA, Wang Z-, Hsiao BS. Secondary structure and elevated temperature crystallite morphology of nylon-6/layered silicate nanocomposites. *Polymer.* 2001; **42:** 1621-1631.

[15] Fong H, Liu W, Wang CS, Vaia RA. Generation of electrospun fibers of nylon 6 and nylon 6-montmorillonite nanocomposite. *Polymer.* 2002; **43:** 775-780.

[16] Fornes TD, Paul DR. Crystallization behavior of nylon 6 nanocomposites. *Polymer.* 2003; **44:** 3945-3961.

[17] Li L, Bellan LM, Craighead HG, Frey MW. Formation and properties of nylon-6 and nylon-6/montmorillonite composite nanofibers. *Polymer.* 2006; **47:** 6208-6217.

[18] Liang Y, Xia X, Luo Y, Jia Z. Synthesis and performances of Fe2O3/PA-6 nanocomposite fiber. *Mater. Letts.* 2007; **61:** 3269-3272.

[19] Cadek M, Le Foulgoc B, Coleman JN, Barron V, Sandler J, Shaffer MSP, Fonseca A, van Es M, Schulte K, Blau WJ. Mechanical and thermal properties of CNT and CNF reinforced polymer composites. *AIP Conference Proceedings.* 2002; 562-565.

[20] Wu S, Wang F, Ma CM, Chang W, Kuo C, Kuan H, Chen W. Mechanical, thermal and morphological properties of glass fiber and carbon fiber reinforced polyamide-6 and polyamide-6/clay nanocomposites. *Mater. Letts.* 2001; **49:** 327-333.

[21] Akkapeddi MK, Glass fiber reinforced polyamide-6 nanocomposites. *Polym. Compos.* 2000; **21:** 576-585.

[22] Vlasveld DPN, Bersee HEN, Picken SJ. Nanocomposite matrix for increased fibre composite strength. *Polymer.* 2005; **46:** 10269-10278.

[23] Vlasveld DPN, Parlevliet PP, Bersee HEN, Picken SJ. Fibre–matrix adhesion in glass-fibre reinforced polyamide-6 silicate nanocomposites. *Compos. Part A.* 2005; **36:** 1-11.

[24] van Rijswijk K, Lindstedt S, Vlasveld DPN, Bersee HEN, Beukers A. Reactive processing of anionic polyamide-6 for application in fiber composites: A comparitive study with melt processed polyamides and nanocomposites. *Polym. Testing.* 2006; **25:** 873-887.

[25] Sandler JKW, Pegel S, Cadek M, Gojny F, van Es M, Lohmar J, Blau WJ, Schulte K, Windle AH, Shaffer MSP. A comparative study of melt spun polyamide-12 fibres reinforced with carbon nanotubes and nanofibres. *Polymer.* 2004; **45:** 2001-15.

[26] Jawahar P, Balasubramanian M. Influence of nanosize clay platelets on the mechanical properties of glass fiber reinforced polyester composites. *J. Nanosci. Nanotechnol.* 2006; **6:** 3973-3976.

[27] Chandradass J, Kumar MR, Velmurugan R. Effect of nanoclay addition on vibration properties of glass fibre reinforced vinyl ester composites. *Mater. Letts.* 2007; **61:** 4385-4388

[28] See ,*http://nano-lab.com/productdatasheets.html.*

[29] Poulin P, Vigolo B, Launois P. Films and fibers of oriented single wall nanotubes. *Carbon.* 2002; **40:** 1741-1749.

[30] Koerner H, Price G, Pearce NA, Alexander M, Vaia RA. Remotely actuated polymer nanocomposites - Stress-recovery of carbon-nanotube-filled thermoplastic elastomers. *Nature Mater.* 2004; **3:** 115-120.

[31] Sen R, Bin Zhao, Perea D, Itkis ME, Hui Hu, Love J, Bekyarova E, Haddon RC. Preparation of single-walled carbon nanotube reinforced polystyrene and polyurethane nanofibers and membranes by electrospinning. *Nano Letts.* 2004; **4:** 459-64.

[32] Chen W, Tao X, Liu Y. Carbon nanotube-reinforced polyurethane composite fibers. *Compos. Sci. Technol.* 2006; **66:** 3029-3034.

[33] Demir MM, Yilgor I, Yilgor E, Erman B. Electrospinning of polyurethane fibers. *Polymer.* 2002; **43:** 3303-3309.

[34] Roy S, Vengadassalam K, Hussain F, Lu H. Compressive strength enhancement of pultruded thermoplastic composites using nanoclay reinforce. In: 49th International SAMPE Symposium and Exhibition: Materials and Processing Technology - 60 Years of SAMPE Progress, SAMPE 2004. May 16-20 2004; Long Beach, CA, United States; 2004:2245-2259.

[35] Kumar S, Doshi H, Srinivasarao M, Park JO, Schiraldi DA. Fibers from polypropylene/nano carbon fiber composites. *Polymer.* 2002; **43:** 1701-1703.

[36] Zhang S, Hull TR, Horrocks AR, Smart G, Kandola BK, Ebdon J, Joseph P, Hunt B. Thermal degradation analysis and XRD characterisation of fibre-forming synthetic polypropylene containing nanoclay. *Polym. Degrad. Stabil.*2007; **92:**727-732

[37] Ruan SL, Gao P, Yang XG, Yu TX. Toughening high performance ultrahigh molecular weight polyethylene using multiwalled carbon nanotubes. *Polymer.* 2003; **44:** 5643-5654.

[38] Ruan S, Gao P, Yu TX. Ultra-strong gel-spun UHMWPE fibers reinforced using multiwalled carbon nanotubes. *Polymer.* 2006; **47:** 1604-1611.

[39] Denchev Z, Oliveira MJ, Mano JF, Viana JC, Funari SS. Nanostructured composites based on polyethylene - polyamide blends. II. Probing the orientation in polyethylene - polyamide

nanocomposites and their precursors. In: European Physical Society Macromolecular Conference - Synchrotron Radiation in Polymer Science 2. 4-6 Sept. 2002; Sheffield, UK: Marcel Dekker; 2004:163-76.

[40] Ji Y, Li B, Ge S, Sokolov JC, Rafailovich MH. Structure and Nanomechanical Characterization of Electrospun PS/Clay Nanocomposite Fibers. *Langmuir.* 2006; **22:** 1321-1328.

[41] Qian D, Dickey EC, Andrews R, Rantell T. Load transfer and deformation mechanisms in carbon nanotube-polystyrene composites. *Appl. Phys. Lett.* 2000; **76:** 2868-2870.

[42] Dror Y, Salalha W, Khalfin RL, Cohen Y, Yarin AL, Zussman E. Carbon Nanotubes Embedded in Oriented Polymer Nanofibers by Electrospinning. *Langmuir.* 2003; **19:** 7012-7020.

[43] Zeng J, Kumar S, Iyer S, Schiraldi DA, Gonzalez RI. Reinforcement of poly(ethylene terephthalate) fibers with polyhedral oligomeric silsesquioxanes (POSS). *High Perform. Polym.* 2005; **17:** 403-24.

[44] Jen MR, Tseng Y, Wu C. Manufacturing and mechanical response of nanocomposite laminates. *Compos. Sci. Technol.* 2005; **65:** 775-779.

[45] Sandler J, Werner P, Shaffer MSP, Demchuk V, Altstädt V, Windle AH. Carbon-nanofibre-reinforced poly(ether ether ketone) composites. *Composites Part A: Appl .Sci. Manufactur.* 2002; **33:** 1033-1039.

[46] Schmidt H, Multifunctional inorganic-organic composite sol-gel coatings for glass surfaces. *J. Non-Crystalline Solids.* 1994; **178:** 302-312.

[47] Lin J, In situ syntheses and phase behavior investigations of inorganic materials in orgamic polymer solid matrices. PhD dissertation, Department of Chemistry, The Pennsylvania State University; 1992. .

[48] Wang Q, Xue Q, Liu W, Chen J. The friction and wear characteristics of nanometer SiC and polytetrafluoroethylene filled polyetheretherketone. *Wear.* 2000; **243:** 140-146.

[49] Ogasawara T, Ishida Y, Ishikawa T, Yokota R. Characterization of multi-walled carbon nanotube/phenylethynyl terminated polyimide composites. *Compos. Part A.* 2004; **35:** 67-74.

[50] Fu HJ, Huang YD, Liu L. Influence of fibre surface oxidation treatment on mechanical interfacial properties of carbon fibre/polyarylacetylene composites. *Mater. Sci. Technol.* 2004; **20:** 1655-1660.

[51] Zhang X, Huang Y, Wang T, Liu L. Influence of fibre surface oxidation–reduction followed by silsesquioxane coating treatment on interfacial mechanical properties of carbon fibre/polyarylacetylene composites. *Compos Part A.* 2007; **38:** 936-944.

[52] Lin Z, Ye W, Du K, Zeng H. Homogenization of functional groups on surface of carbon fiber and its surface energy. *J Huaqiao Univ.* 2001; **22:** 261-263.

[53] Zhang X, Huang Y, Wang T, Hu L. Influence of oligomeric silsesquioxane coatings treatment on the interfacial property of CF/PAA composites. *Acta Mater. Compos. Sinica.* 2006; **23:** 105-111.

[54] Kumar S, Dang TD, Arnold FE, Bhattacharyya AR, Min BG, Zhang X, Vaia RA, Park C, Adams WW, Hauge RH, Smalley RE, Ramesh S, Willis PA. Synthesis, structure, and properties of PBO/SWNT composites. *Macromolecules.* 2002; **35:** 9039-9043.

Caption of Figures

Figure 1 Modulus us. density of glass fibre (GF), PA-6/nanoclay (PA-6/NC) vs. PA-6 moulding resins [21].

Figure 2 Flexural strength of carbon fibre composites with PA6, a commercially available PA6 nanocomposite (Unitika M1030D from Unitika) and nanocomposite matrix as a function of the matrix modulus (dry and moisture conditioned) [23].

Figure 3 Infusion equipment - from left to right: Mini Mixing Unit "MMU-TU Delft", resin reservoir, stainless steel infusion mould, resin trap, cold trap and vacuum pump [24].

Figure 4 Pressure-temperature profile of the curing process of AS-4/PEEK APC-2 nanocomposites [44]

Figure 5 Effect of the multi-walled carbon nanotubes concentration on Young's modulus of the composites [49].

Figure 6 Schematic diagrams of carbon fibre treatment process (sample 1 is oxygen plasma oxidation, sample 2 is $LiAlH_4$ reduction, sample 3 is VMS–SSO coating) [51].

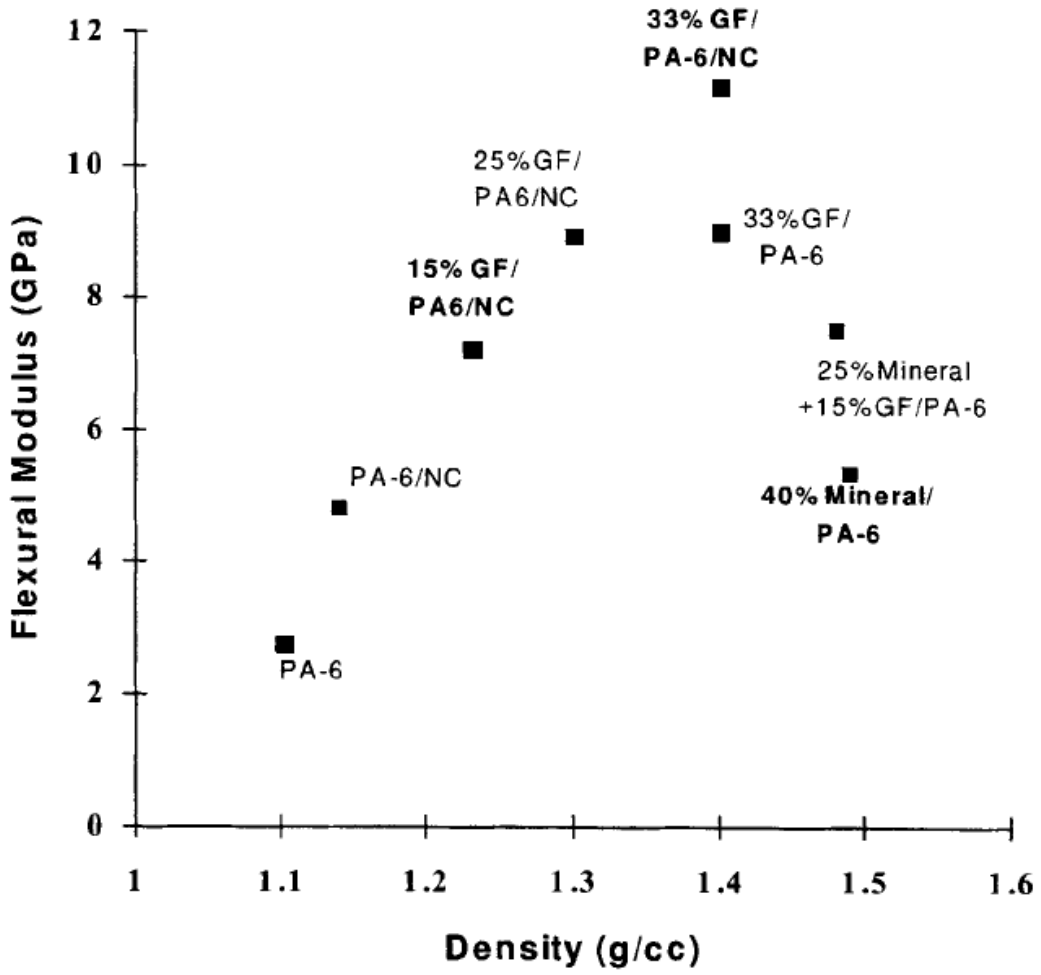

Figure 1 Modulus us. density of glass fibre (GF), PA-6/nanoclay (PA-6/NC) vs. PA-6 moulding resins [21].

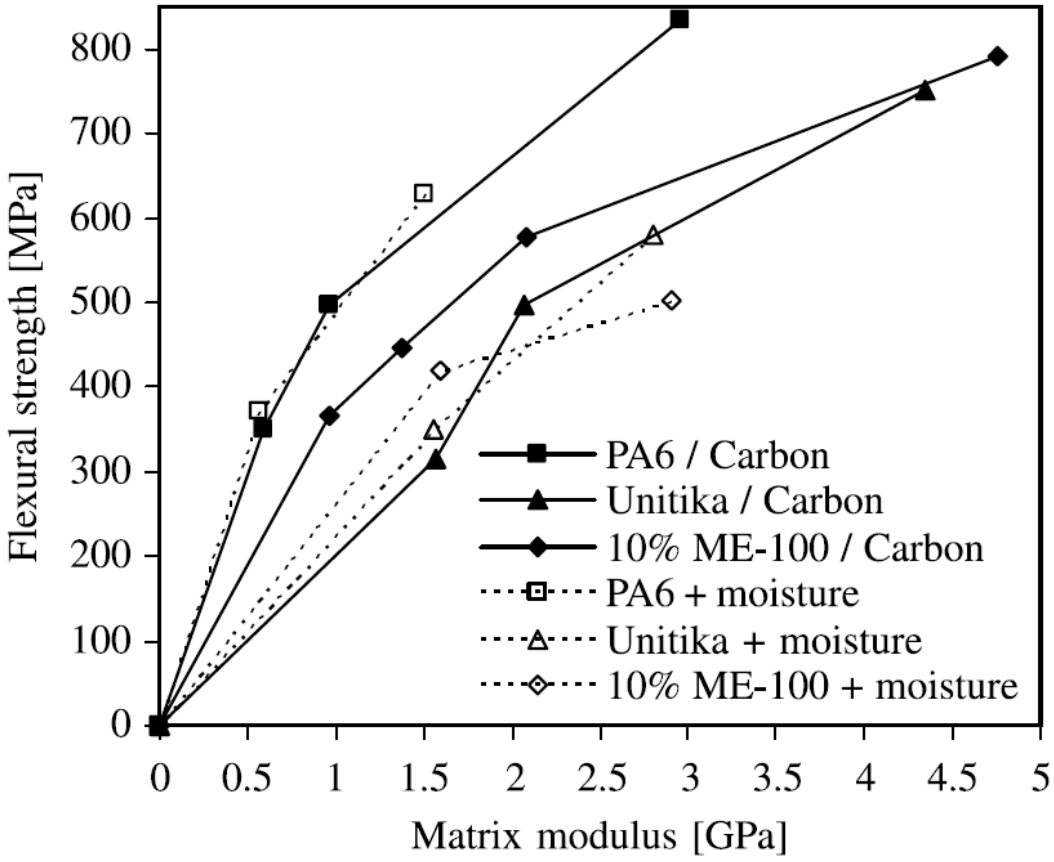

Figure 2 Flexural strength of carbon fibre composites with PA6, a commercially available PA6 nanocomposite (Unitika M1030D from Unitika) and nanocomposite matrix as a function of the matrix modulus (dry and moisture conditioned) [23].

Figure 3 Infusion equipment - from left to right: Mini Mixing Unit "MMU-TU Delft", resin reservoir, stainless steel infusion mould, resin trap, cold trap and vacuum pump [24]**.**

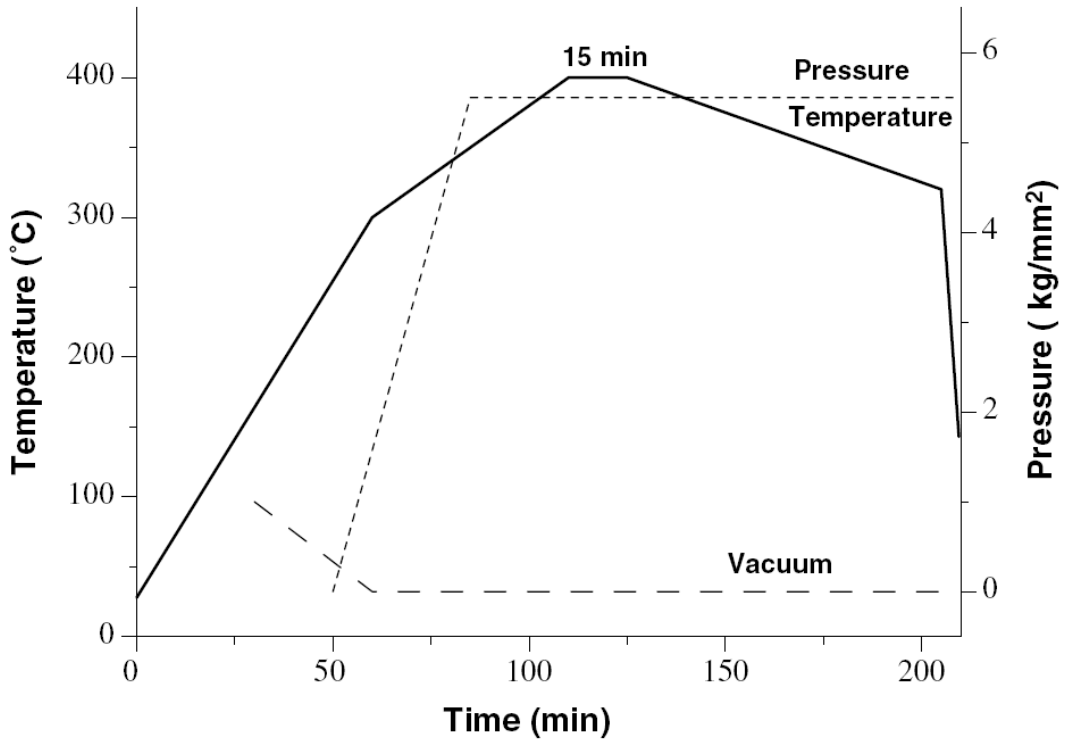

Figure 4 Pressure-temperature profile of the curing process of AS-4/PEEK APC-2 nanocomposites [44]

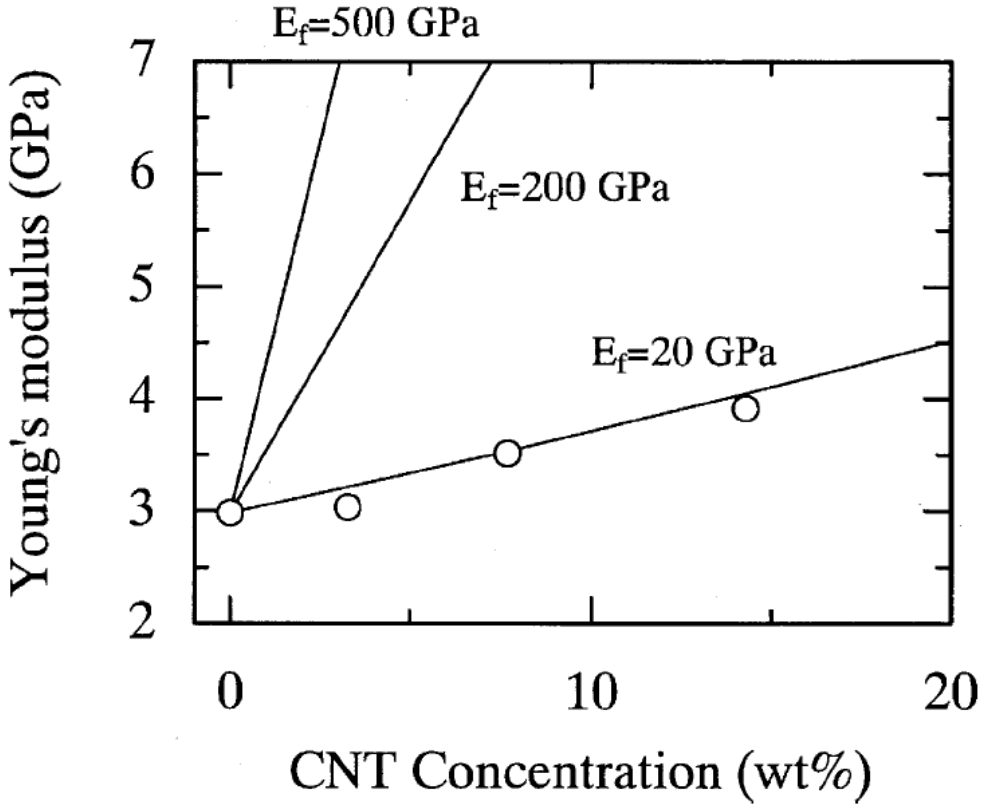

Figure 5 Effect of the multi-walled carbon nanotubes concentration on Young's modulus of the composites [49].

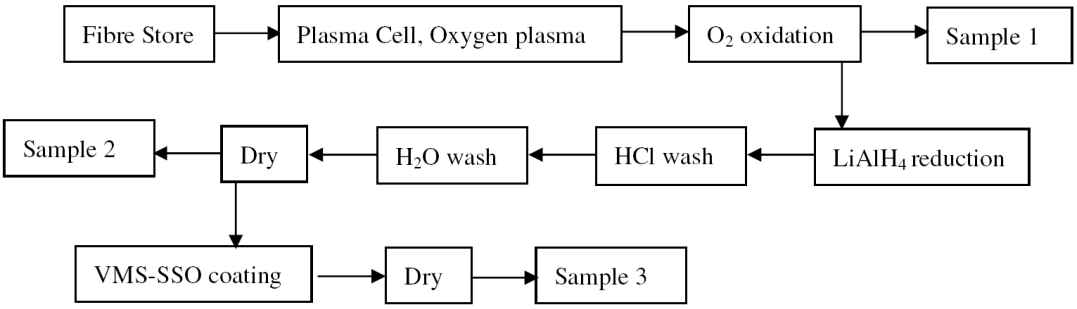

Figure 6 Schematic diagrams of carbon fibre treatment process (sample 1 is oxygen plasma oxidation, sample 2 is $LiAlH_4$ reduction, sample 3 is VMS–SSO coating) [51].